

## Recovery of microstructure and surface topography of grinding-damaged silicon wafers by nanosecond-pulsed laser irradiation

This content has been downloaded from IOPscience. Please scroll down to see the full text.

2009 Semicond. Sci. Technol. 24 105018

(<http://iopscience.iop.org/0268-1242/24/10/105018>)

View [the table of contents for this issue](#), or go to the [journal homepage](#) for more

Download details:

IP Address: 131.113.58.246

This content was downloaded on 26/06/2015 at 09:02

Please note that [terms and conditions apply](#).

# Recovery of microstructure and surface topography of grinding-damaged silicon wafers by nanosecond-pulsed laser irradiation

Jiawang Yan<sup>1,3</sup>, Shin Sakai<sup>2</sup>, Hiromichi Isogai<sup>2</sup> and Koji Izunome<sup>2</sup>

<sup>1</sup> Department of Nanomechanics, Graduate School of Engineering, Tohoku University, Aramaki Aoba 6-6-01, Aoba-ku, Sendai 980-8579, Japan

<sup>2</sup> Covalent Materials Corporation, 6-861-5 Higashiku, Seirou-machi, Kitakanbara-gun, Niigata 957-0197, Japan

E-mail: [yanjw@pm.mech.tohoku.ac.jp](mailto:yanjw@pm.mech.tohoku.ac.jp)

Received 19 May 2009, in final form 29 July 2009

Published 18 September 2009

Online at [stacks.iop.org/SST/24/105018](http://stacks.iop.org/SST/24/105018)

## Abstract

Single crystalline silicon wafers whose surfaces were machined by diamond grinding were irradiated by a nanosecond-pulsed Nd:YAG laser. Changes in the subsurface crystallinity and surface topography were investigated by transmission electron microscopy and atomic force microscopy. It was found that the grinding process gave rise to amorphous layers, dislocations and micro cracks. However, all of this damage could be eliminated by a single laser pulse of suitable energy density, which also led to a remarkable amount of smoothing of the wafer surface. When excessively high energy densities were used, tiny particles were found to form on the wafer surface. It is speculated that these particles are produced by the recondensation of silicon boiled away from the wafer surface during the laser pulse. The temperature rise during laser irradiation was estimated using a simplified model. The results obtained in this study suggest that nanosecond-pulsed laser irradiation may be an effective approach for processing grinding-damaged silicon wafers.

(Some figures in this article are in colour only in the electronic version)

## 1. Introduction

Silicon wafers used for the fabrication of ultra-large-scale integration (ULSI) devices are usually manufactured by mechanical and chemical processes such as slicing, lapping, grinding, etching and polishing. The mechanical processes inevitably cause subsurface damage, such as microstructural changes and the introduction of dislocations, to the silicon substrates [1–5], and removal of this damage is essential for producing reliable devices. In conventional rough grinding processes, micro cracks generated beneath the wafer surface may extend to a depth of  $\sim 10 \mu\text{m}$ , or much deeper. To completely remove such a thick subsurface damage layer, chemical etching and chemo-mechanical polishing (CMP)

processes are necessary. In recent years, however, the ductile mode grinding (DMG) technique has been developed and widely used for precision machining of silicon wafers [6, 7]. In DMG, by using ultraprecision grinding machines and grinding wheels with extremely fine diamond abrasives, no micro cracks will be generated in the wafers. In this case, the grinding-induced subsurface damage layer will be extremely thin, consisting of an amorphous layer (depth  $\sim$  a few tens of nanometers) and dislocations (depth  $\sim$  a few hundreds of nanometers). To further improve the quality of such precision-machined silicon wafers in place of etching and chemo-mechanical polishing, an alternative method currently being considered is the use of laser irradiation. In a previous paper [8], Yan *et al* demonstrated the feasibility of recovering the lattice structure of diamond-cut silicon wafers by using a nanosecond-pulsed Nd:YAG laser. The subsurface structure

<sup>3</sup> Author to whom any correspondence should be addressed.

recovery mechanism involved the sudden melting of the damaged layer and the subsequent epitaxial regrowth from the damage-free bulk during cooling [8]. In comparison with chemo-mechanical or chemical processes, laser irradiation offers a number of advantages: (i) it involves no removal of material, thus preserving the dimensions of the workpiece; (ii) it generates no pollutants; (iii) it enables selective processing and processing of complex shapes.

In this paper, silicon wafers machined by ultraprecision diamond grinding were used as specimens for laser irradiation tests. Such grinding is a very important technical step in the current silicon wafer manufacturing process [9]. In contrast to single-point diamond cutting, the grinding process gives rise to non-uniform subsurface damage layers with complicated microstructures. In addition, significant grinding marks and surface waviness may be produced. Therefore, two effects are expected during laser processing of ground wafers: one is an improvement in the subsurface integrity, and the other is the smoothing of the grinding marks. In this paper, the response of precisely diamond-ground silicon wafers to a nanosecond-pulsed Nd:YAG laser was experimentally investigated. The effects of laser energy density on the changes in the subsurface structure and surface topography of the wafers were examined.

## 2. Experimental procedures

Boron-doped p-type device-grade single-crystal silicon (100) wafers machined by diamond grinding were used as specimens in this study. The grinding procedure was carried out with an ultraprecision grinder equipped with vitrified grinding wheels with fine diamond abrasives. The average size of the abrasive grains was approximately 2  $\mu\text{m}$ .

The machined sample was then irradiated by a Nd:YAG laser machining system, QuikLaze-50, produced by New Wave Research, Inc. (Fremont, USA). This system employs a flash lamp pumped Nd:YAG rod in a thermally compensated three bar invar resonator to generate radiation at 1064 nm. The 1064 nm laser pulse was passed through an angle-tuned KTP crystal to generate a second harmonic at 532 nm. The laser beam was shaped to a rectangle using XY apertures, and after passing through an objective lens a maximum beam width of  $50 \times 50 \mu\text{m}^2$  was obtained. In the present experiment, the XY apertures were both set to 40%, producing a  $20 \times 20 \mu\text{m}^2$  square irradiation area. A single pulse mode was used and the pulse width was 3–4 ns. The incident energy of each laser pulse was varied from 0.96 to 5.76  $\mu\text{J}$ , leading to a change in energy intensity from 0.24 to 1.44  $\text{J cm}^{-2}$ . The laser irradiation conditions are summarized in table 1.

To investigate the changes in the subsurface microstructure resulting from laser irradiation, cross-sectional observations of the sample were performed using transmission electron microscopy (TEM). The instrument used was an H-9000UHRIII, produced by Hitachi Ltd (Tokyo, Japan). The acceleration voltage was 300 kV. To prepare the TEM samples, the silicon wafers were processed by ion milling using a Dual Mill 600 system (Gatan, Inc., USA). To protect the sample from possible damage during ion milling, a carbon coating was deposited on the surface.

**Table 1.** Laser irradiation conditions.

Laser type	Nd:YAG
Wavelength	532 nm
Pulse width	3–4 ns
Pulse mode	Single pulse
Irradiation area	$20 \times 20 \mu\text{m}^2$
Energy density	0.24–1.44 $\text{J cm}^{-2}$
Environment	In air

To determine surface topographical changes, the sample surface was characterized using an atomic force microscope (AFM) Nanoscope IIIa (Veeco Instruments, USA). The AFM measurements were performed within a  $10 \times 10 \mu\text{m}^2$  square area under a tapping mode. Five samples were made for each laser irradiation condition, and two of them were taken for TEM observation. Surface roughness measurement was performed for all the samples.

## 3. Results

### 3.1. Subsurface structural changes

Figure 1(a) shows a cross-sectional TEM micrograph of a silicon wafer, where the left side is a region without laser irradiation and the right side was irradiated at a low energy density of 0.72  $\text{J cm}^{-2}$ . Figures 1(b) and (c) are close-up views of the unirradiated and the irradiated region, respectively, as indicated in figure 1(a). From figure 1(b), it can be seen that severe subsurface damage has resulted from the grinding process, leading to the formation of both an amorphous layer and a dislocated layer. In contrast to diamond-cut samples [5, 8] where the subsurface damage depth was uniform, the depths of both the amorphous layer and the dislocation layer in figure 1(b) vary greatly from place to place. The total thickness of the damage layer ranges from approximately 50 nm to 150 nm. From figures 1(a) and (b), it can be seen that before laser irradiation the surface unevenness corresponding to the grinding marks is approximately 40 nm, which is much rougher than that of the diamond-cut surface [5, 8]. After laser irradiation (figure 1(c)), the amorphous layer has disappeared and the surface unevenness has been reduced slightly. In addition, the number of dislocations has decreased distinctly and a few regions have become damage-free. Therefore, it can be said that under this laser irradiation condition, grinding-induced subsurface damage has been partially removed.

Figure 2(a) shows a cross-sectional TEM micrograph of a sample where the left side was unirradiated and the right side was irradiated at a high energy density of 1.44  $\text{J cm}^{-2}$ . Figures 2(b) and (c) are high-magnification images of the two regions indicated in figure 1(a). As before, the subsurface damage in the unirradiated region includes an amorphous layer and a dislocated layer. Also, several sharp protrusions of dislocations into the substrate could be observed, which are presumably potential micro cracks. However, after laser irradiation, all grinding damage including the amorphous layer, the dislocations and the micro cracks, have disappeared completely, and the near-surface layer has the same structure as the bulk region. From figure 2(c), it is also evident that

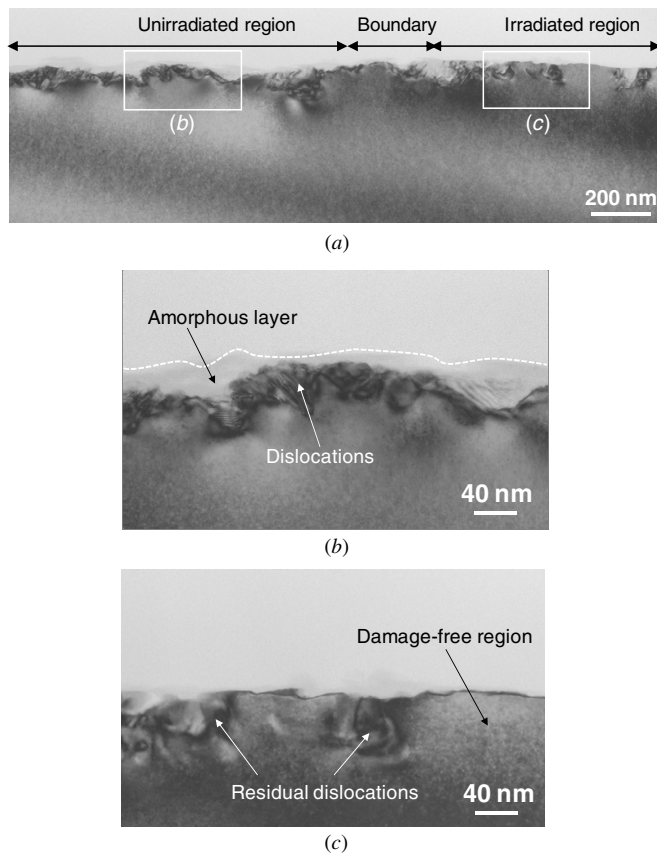


**Figure 1.** Cross-sectional TEM micrographs of a silicon wafer: (a) a general view showing the unirradiated region on the left side and the laser irradiated region on the right side. The laser energy density was  $0.72 \text{ J cm}^{-2}$ ; (b) and (c) are close-up views of the regions indicated by the white lines in (a).

after laser irradiation the wafer surface has become distinctly smoother than that of the unirradiated region (figure 2(b)) and that of the specimen irradiated at the low energy density (figure 1(c)).

### 3.2. Surface topographical changes

Next, the changes in surface topography were investigated using AFM. Figures 3(a)–(e) show AFM images of the wafer surface before and after laser irradiation at different energy densities. As shown in figure 3(a), before laser irradiation numerous parallel grinding marks, a few tens of nanometers in height and several hundreds of nanometers in width, are clearly seen on the surface. These are obviously the result of the single-point cutting and scratching effects of the diamond abrasive grains. After laser irradiation at an energy density of  $0.48 \text{ J cm}^{-2}$ , no obvious change in surface topography could be detected, as shown in figure 3(b). However, at a higher energy density of  $0.72 \text{ J cm}^{-2}$ , a few fine grinding marks disappeared and the surface became significantly flatter, as shown in figure 3(c). When the energy density was further increased to  $1.04 \text{ J cm}^{-2}$  (figure 3(d)), a further large increase in surface smoothness occurred, while a few sub-micron-sized particles began to appear on the surface. Figure 3(e) shows the result obtained at an energy density of  $1.44 \text{ J cm}^{-2}$ ,

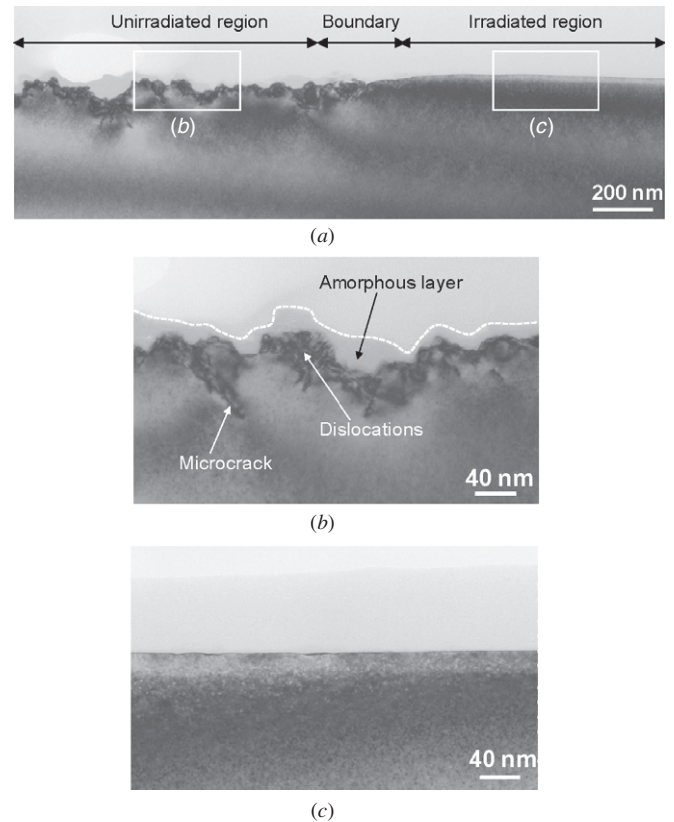


**Figure 2.** Cross-sectional TEM micrographs of a silicon wafer: (a) a general view showing the unirradiated region on the left side and the laser irradiated region on the right side. The laser energy density was  $1.44 \text{ J cm}^{-2}$ ; (b) and (c) are close-up views of the regions indicated by the white lines in (a).

where it can be seen that both the number and the size of the small particles have increased slightly in comparison with figure 3(d).

Figure 4 shows a plot of surface roughness against laser energy density. The surface roughness was calculated as the root mean square (RMS) value of the three-dimensional AFM topography data. The surface roughness before laser irradiation was  $\sim 12 \text{ nm}$ . At a laser energy density of  $0.72 \text{ J cm}^{-2}$ , it shows a sudden decrease to  $\sim 8 \text{ nm}$ . However, it began to increase again from an energy density of  $1.04 \text{ J cm}^{-2}$ . This increase at higher energy densities was found to be due to the presence of the small particles. After recalculation following removal of the data points corresponding to the biggest twenty particles, the surface roughness became similar to or smaller than that obtained at an energy density of  $0.72 \text{ J cm}^{-2}$ , as indicated by triangles in figure 4.

## 4. Discussion

The mechanism of surface topographical and subsurface microstructural changes during laser irradiation has not yet been completely clarified. It is presumed that the recovery of the subsurface structure may be the result of sudden melting of the surface layer and subsequent epitaxial regrowth during cooling [8]. A similar phenomenon has been confirmed in conventional laser annealing processes

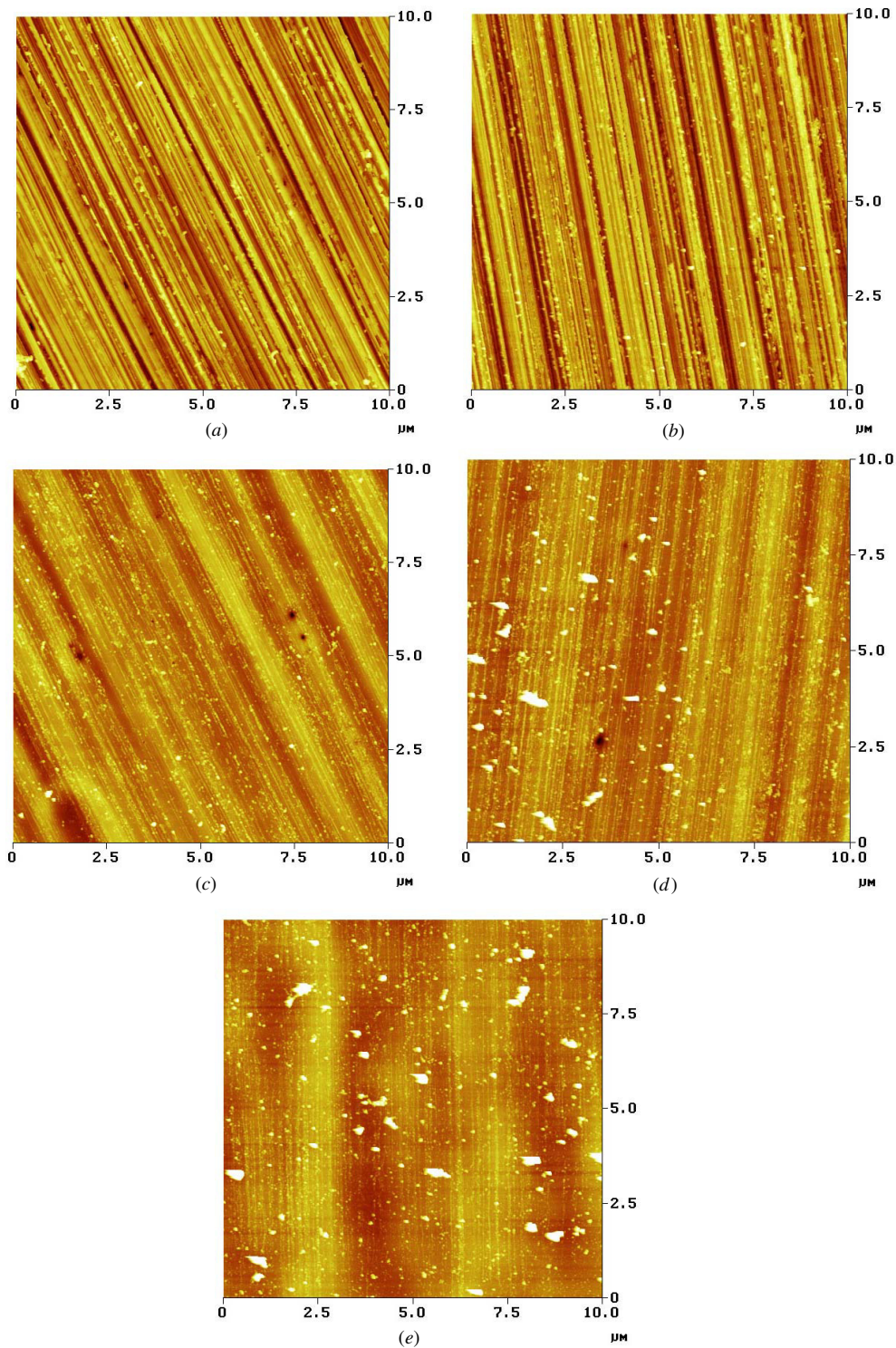


**Figure 3.** AFM images of the wafer surface (a) before laser irradiation and after laser irradiation at different energy density levels: (b) 0.48, (c) 0.72, (d) 1.04 and (e) 1.44 J cm<sup>-2</sup>.

[10–14]. Since amorphous silicon has a much higher light absorption coefficient than crystalline silicon, there is likely to be sufficient absorption of laser energy in the near-surface layer to form a thin liquid silicon film. The liquid layer is metallic and strongly absorbs laser energy, thus becoming thicker and thicker. The top-down melted liquid phase finally extends to below the dislocated region. After the laser

pulse, environmental cooling will result in bottom-up epitaxial regrowth from the defect-free substrate [8]. In this way, a perfect single crystalline structure can be obtained in the surface region. This epitaxial regrowth mechanism is different from that involved in the laser annealing of silicon layers on substrates such as glass and sapphire, where no lattice-matched crystal seed exists.

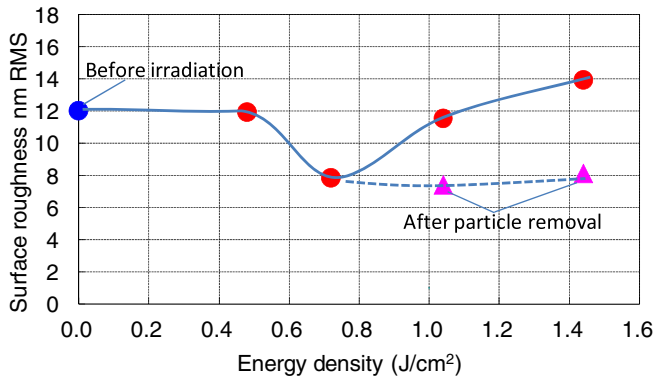


**Figure 4.** Plot of surface roughness (RMS) versus laser energy density.

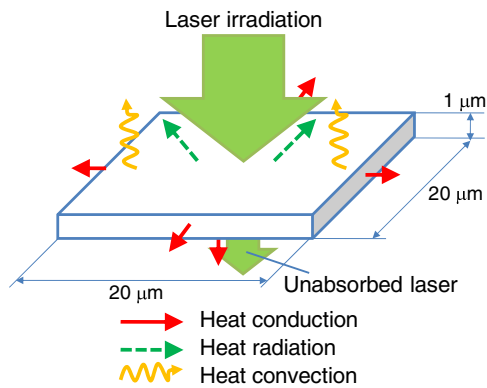


**Figure 5.** Simplified model for calculating the temperature rise due to laser irradiation.

The melting of silicon has been confirmed in the conventional laser annealing process by measuring the time-resolved optical reflectivity [13] or by detecting the presence/absence of oxygen thermal donors and oxidation-induced stacking faults [14]. In this work, it was difficult for the authors to directly detect the melting phenomenon. Instead, we made a rough estimation of laser-induced temperature rise using a simplified model shown in figure 5, since the melting of silicon depends on the surface temperature rise. It is first supposed that a fraction of the energy of the laser beam will be uniformly absorbed by a small volume of material with dimensions  $20 \times 20 \times 1 \mu\text{m}^3$  on the wafer surface ( $20 \times 20 \mu\text{m}^2$  is the area of the laser irradiated region, and  $1 \mu\text{m}$  is the penetration depth of the 532 nm Nd:YAG laser into silicon [15]). Then, the temperature rise ( $\Delta T$ ) in this small volume can be described by the following equation:

$$\Delta T = \frac{Q \cdot \eta}{c \cdot M} = \frac{E \cdot S \cdot \eta}{c \cdot M}, \quad (1)$$

where  $Q$  is the total quantity of heat generated by the laser irradiation,  $\eta$  is the energy absorption ratio of the volume taking into account the heat lost by conduction, radiation and convection,  $E$  is the energy density of the laser,  $S$  is the area of the irradiated region,  $c$  is the specific heat of silicon and  $M$  is the mass of the material within the small volume. In this paper, these parameters were assigned the following values:  $E = 0\text{--}1.60 \text{ J cm}^{-2}$ ,  $S = 4.0 \times 10^{-6} \text{ cm}^2$ ,  $c = 680.4 \text{ J }^\circ\text{C}^{-1} \text{ kg}^{-1}$ ,  $M = 9.32 \times 10^{-13} \text{ kg}$ . A rough

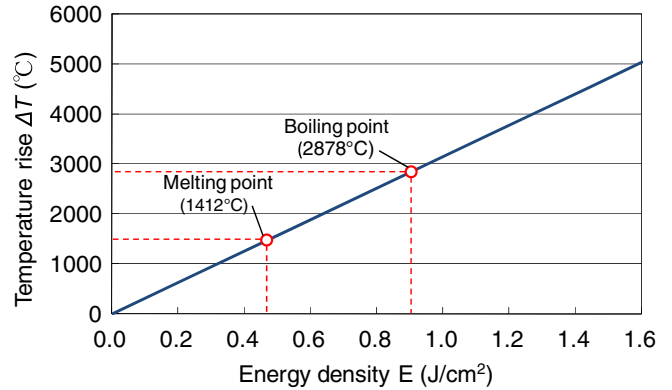


**Figure 6.** Plot of the calculated temperature rises against energy density.

approximation of  $\eta \approx 0.5$  was made by considering the laser absorption coefficients of single crystalline and amorphous silicon, respectively, and the heat loss due to conduction, radiation and convection. A detailed analysis of laser absorption and heat transfer will be presented in a future paper.

The calculated temperature rise as a function of energy density is plotted in figure 6. It can be seen that at an energy density of  $0.48 \text{ J cm}^{-2}$ , the temperature rise is  $1514 \text{ }^\circ\text{C}$ , which is higher than the melting point of silicon ( $1412 \text{ }^\circ\text{C}$ ). This result generally agrees with the experimental result that the surface roughness of the wafer decreased after laser irradiation at an energy density level higher than  $0.48 \text{ J cm}^{-2}$ . This fact, to some extent, demonstrated the validity of the estimation model we used. In figure 6, when the energy density is increased to  $0.96 \text{ J cm}^{-2}$ , the temperature rise becomes  $3028 \text{ }^\circ\text{C}$ , which is higher than the boiling point of silicon ( $2878 \text{ }^\circ\text{C}$ ) [16]. From this result, it is suggested that if the laser energy density is sufficiently high, silicon on the surface can boil and be scattered as small droplets. These droplets, after the laser pulse has terminated, would be reattached to the surface forming tiny particles. These surface particles can be completely removed by slightly performing polishing after laser irradiation.

It should be pointed out that parameters used in the analysis, such as the energy absorption ratio, may not be quantitatively accurate. Also, an assumption was made that energy absorption was uniform within the small volume, and this may not be the case in reality. Therefore, the results of the calculations presented here must be considered as a starting point only. Further work is necessary to improve the model and its parameters. Also, further experiments are needed to find the optimum laser irradiation conditions to cause the silicon surface to melt without boiling, so that the damage layer can be recovered without the formation of unwanted particles. In that case, the laser processed wafer surface will be as smooth as the polished one, and there will be no need for further polishing.

An important finding from the present study is the ability of laser irradiation to smooth the silicon surface. The driving force for the smoothing effect might be the surface tension of the melted silicon thin film. Similar to the manner in which a free droplet of liquid naturally assumes a spherical shape to achieve a minimum surface area to volume ratio, in this study the surface area reaches a minimum when the silicon

liquid becomes completely flat. Since the proposed technique offers the combined advantages of damage removal and surface smoothing, it has considerable potential as a single step process to improve the near-surface quality of silicon wafers.

## 5. Conclusions

Diamond-ground silicon wafers were irradiated by a nanosecond-pulsed laser and changes in the subsurface structure and surface topography were investigated. The main conclusions can be summarized as follows.

- (1) The grinding process was found to give rise to an amorphous layer on the silicon surface in addition to dislocations and potential micro cracks. The total thickness of the subsurface damage layer varied from approximately 50 nm to 150 nm.
- (2) Following a single laser pulse at a sufficiently high energy density ( $\sim 1.44 \text{ J cm}^{-2}$ ), subsurface defects were completely eliminated and a single-crystal structure was recovered.
- (3) Grinding marks were smoothed significantly after laser irradiation, leading to a decrease in RMS surface roughness from  $\sim 12$  to  $\sim 8$  nm.
- (4) At high energy densities ( $> 1.04 \text{ J cm}^{-2}$ ), small particles were formed on the wafer surface. It is speculated that these are generated by the boiling and scattering of liquid silicon droplets.

## Acknowledgment

This work has been supported in part by a grant-in-aid for Exploratory Research (project no 20656023) from the Japan Society for the Promotion of Science (JSPS).

## References

- [1] Shibata T, Ono A, Kurihara K, Makino E and Ikeda M 1994 *Appl. Phys. Lett.* **65** 2553–5
- [2] Puttick K E, Whitmore L C, Chao C L and Gee A E 1994 *Phil. Mag. A* **69** 91–103
- [3] Gogotsi Y, Baek C and Kirscht F 1999 *Semicond. Sci. Technol.* **14** 936–44
- [4] Yan J 2004 *J. Appl. Phys.* **95** 2094–101
- [5] Yan J, Asami T and Kuriyagawa T 2007 *Precis. Eng.* **32** 186–95
- [6] Noboru M 2000 Microscopic mechanism of ductile mode grinding of silicon wafer *J. Japan. Soc. Abrasive Technol.* **44** 426–8
- [7] Klocke F and Pähler D 2001 Precision machining of future silicon wafers *Initiatives of Precision Engineering at the Beginning of a Millennium Proc. of the 10th International Conf. on Precision Engineering (ICPE) (Yokohama, Japan, 18–20 July 2001)* (Berlin: Springer) pp 411–5
- [8] Yan J, Asami T and Kuriyagawa T 2007 *Semicond. Sci. Technol.* **22** 392–5
- [9] Pei Z J, Li Z C and Fisher G R 2007 Grinding of silicon wafers in the nanotechnology era *Semiconductor Machining at the Micro–Nano Scale* ed J Yan and J Patten (Kerala, India: Transworld Research Network) pp 219–41
- [10] Bean J C, Leamy H J, Poate J M, Rozgonyi G A, Sheng T T, Williams J S and Celler G K 1978 *Appl. Phys. Lett.* **33** 227
- [11] Venkatesan T N C, Golovchenko J A, Poate J M, Cowan P and Celler G K 1978 *Appl. Phys. Lett.* **33** 429
- [12] Murakami K, Gamo K, Namba S, Kawabe M and Aoyagi Y 1979 *Appl. Phys. Lett.* **35** 628
- [13] Lüthy W, Affolter K, Weber H P, Roulet M E, Fallavier M, Thomas J P and Mackowski J 1979 *Appl. Phys. Lett.* **35** 873
- [14] Hayafuji Y, Aoki Y and Usui S 1983 *Appl. Phys. Lett.* **42** 720
- [15] Neuberger M and Wells S J 1969 Silicon Data sheet DS-162 p 110
- [16] Yaws C L, Lutwack R, Dickens L L and Hsu G 1981 *Solid State Technol.* **24** 87–92